# ANALYSIS OF AXISYMMETRIC LAMINATED COMPOSITE SHELLS SUBJECTED TO ASYMMETRIC LOADING

A.R. Upadhya* & KM. Aruna*

**Summary**

A finite *element formulation for the static analysis of a laminated composite shell of revolution with general meridional curvature, subjected to asymmetric loading is presented. The analysis uses an axisymmetric laminated shell element where the shell geometry is satisfactorily represented and higher order polynomial approximations are used for the displacement fields. The asymmetric loading problem is handled through a Fourier series representation of the applied loads and the resultant displacements. Solutions are presented for typical aerospace shell structures like* a *composite cone and a tangent ogive shell subjected to* wind *loads.*

## Introduction

Many aerospace structural configurations are shells of revolution. These shells are often fabricated using fibre reinforced composite materials by the filament winding process or by moulding using several layers of impregnated fabrics. Though the fundamental unit in these constructions is a unidirectional lamina, the overall laminate may be orthotropic, nearly orthotropic or generally anisotropic depending on the number of layers and individual layer orientations. Moreover, eventhough these shells are axisymmetric structures the aerodynamic and inertial loading on them are generally asymmetric. Because of the anisotropic material properties and asymmetric nature of the loading the analysis of these type of shells is usually quite complex.

Most of the analytical formulations available in literature are limited to simple geometrical configurations like cylindrical and conical shells with homogeneous isotropic or orthotropic material properties. The influence of material anisotropy in axisymmetric shells with asymmetric loading has been dealt by Pandovan and Lestingi [1,2]. These authors employ a multisegment numerical integration technique for the solution of shell equilibrium equations using a finite exponential Fourier transform.

The finite element method of analysis provides an alternate simpler method of solution for shells with complex geometries, arbitrary loadings, general boundary conditions and anisotropic material characteristics. Although shells of revolution can be analysed using general shell elements like high precision triangular laminated anisotropic shallow shell element [3], the use of axisymmetric shell elements is simple and attractive for a large class of practical problems [4-8]. However, finite element formulations that take into account orthotropic and anisotropic material properties are limited in number. Reference [9] uses a truncated cone type element (orthotropic) to represent even arbitrary meridional curvatures. Pandovan [10] uses a quasi-analytical finite element procedure with complex Fourier transforms for displacement and force representation for solving the resultant complex displacement equlibrium equations for anisotropic axisymmetric shells.

The analysis presented in this paper uses a finite element procedure based on matrix displacement method. The element employed is a refined axisymmetric shells element specially formulated for the analysis of laminated composite shells of revolution [11]. The asymmetric loading problem is handled through a Fourier series representation of the loads and displacements using a cosine and a sine series for the symmetric and the antisymmetric components respectively. When the shell is isotropic or orthotropic the force-displacement field equations for each harmonic in the series are uncoupled and can be solved separately. However, for a general anisotropic shell, the generalized coordinates corresponding to the sine and cosine series for a given harmonic are coupled and hence will have to be considered together. This leads to doubling of the size of the stiffness matrix and the number of force-displacement equations to be solved. Fortunately for a large number of practical laminated structures, the coupling is zero (i.e. orthotropic) or its effect is smalt. In such cases, effect of the coupling terms can be neglected and solutions obtained for the sine and cosine components in each harmonic seperately.

The finite element method presented in this paper has the following capabilities

1 It can represent a shell with general meridional curvature.

2 Variation of thickness and material properties along the meridian.

* Scientists - National Aeronautical Laboratory Bangalore 560 017

3 Variation of applied loads along the meridian.

4 Loading can be asymmetric.

## 2 Analysis Procedure

### 2.1 Element Description

The element employed is a refined axisymmetric laminated composite shell of revolution element with two nodal circles and seven degrees of freedom per node. A brief description of the element and the development of this formulation are given below.

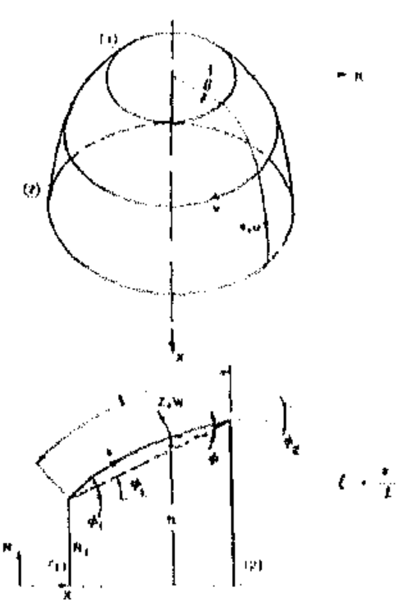

FIG 1. Axisymmetric Shell Element - Geometry and Coordinate System

Fig 1 shows the geometry of the axisymmetric shell finite element and the coordinate system used. The meridional slope is represented as

$$\phi = a_1 + a_2\,\xi + a_3\,\xi^2 \qquad (1)$$

where the coefficients $a_1$, $a_2$ and $a_3$ are given by

$$a_1 = \phi_1$$

$$a_2 = 6\phi_c - 4\phi_1 - 2\phi_2$$

$$a_3 = 3\,(\phi_1 + \phi_2 - 2\phi_c) \qquad (2)$$

These coefficients have been obtained by matching the location and slope of the element with those of the actual shell at the two nodal circles.

The radius r is given by

$$r = R_1 + \int_0^{\xi} \sin[\phi(\xi)]\, d\xi \qquad (3)$$

### 2.2 Displacements

In order to take into account the effect of asymmetric loading the displacements u, v and w at a point on the reference surface of the element are expressed in a general form as a Fourier series expansion in the circumferential coordinate θ as

$$\begin{Bmatrix} u \\ v \\ w \end{Bmatrix} = \begin{Bmatrix} u^{o} \\ v^{o} \\ w^{o} \end{Bmatrix} + \sum_{j=1}^{N_c} \begin{Bmatrix} u^{j}\cos j\theta \\ v^{j}\sin j\theta \\ w^{j}\cos j\theta \end{Bmatrix} + \sum_{j=1}^{N_s} \begin{Bmatrix} \bar{u}^{j}\sin j\theta \\ \bar{v}^{j}\cos j\theta \\ \bar{w}^{j}\sin j\theta \end{Bmatrix} \qquad (4)$$

The element has seven degrees of freedom per node which are the inplane displacement components u and v, their first derivatives in the meridional direction $u_{,s}$ and $v_{,s}$, the out of plane component w and its first and second derivatives $w_{,s}$ and $w_{,ss}$ (subscripts s and ss denote first and second derivatives respectively with respect to s).

The coefficients $u^{o}$, $v^{o}$, $w^{o}$, $u^{j}$, $v^{j}$, $w^{j}$, $\bar{u}^{j}$, $\bar{v}^{j}$, $\bar{w}^{j}$ in the series represented by equation (4) describe the variation in the meridion direction and are interpolated in terms of the generalised displacements at each nodal circle using third order polynomials for u and v, and fifth order polynomial for w.

These relations can be expressed in the general matrix form

$$\{A^{j}\} = [X]\{q^{j}\} \qquad j = 0,1,2,\ldots N_c \qquad (5)$$

$$\{\bar{A}^{j}\} = [X]\{\bar{q}^{j}\} \qquad j = 1,2,3,\ldots N_s \qquad (6)$$

where $\{A^{j}\}$ and $\{\bar{A}^{j}\}$ represent matrices of generalised displacements, $\{q^{j}\}$ and $\{\bar{q}^{j}\}$ matrices of generalized element nodal degrees of freedom, and [X] is a matrix of polynomials in ξ.

$$\{A^{j}\}^{T} = \{u^{j}\ u^{j}_{,s}\ v^{j}\ v^{j}_{,s}\ w^{j}\ w^{j}_{,s}\ w^{j}_{,ss}\}^{T} \qquad (7)$$

and

$$\{q^{j}\}^{T} = \{u^{j}_{1}\ u^{j}_{,s1}\ v^{j}_{1}\ v^{j}_{,s1}\ w^{j}_{1}\ w^{j}_{,s1}\ w^{j}_{,ss1}$$

$$v^{j}_{2}\ v^{j}_{,s2}\ v^{j}_{2}\ v^{j}_{,s2}\ w^{j}_{2}\ w^{j}_{,s2}\ w^{j}_{,ss2}\} \qquad (8)$$

and similarly for $\{\bar{A}^{j}\}$ and $\{\bar{q}^{j}\}$. Matrix [X] is given in Appendix I.

#### Appendix - I

Matrix [X] in the relation $\{A^{j}\} = [X]\{q^{j}\}$

**Non - Zero elements**

X (1,1) X (3,3) $1 - 3\xi^2 + 2\xi^3$

X (1,2) X (3,4) $l(\xi - 2\xi^2 + \xi^3)$

X (1,8) X (3,10) $\xi^2(3 - 2\xi)$

$X(1,9) = X(3,11) = \ell\xi^{2}(\xi-1)$

$X(2,1) = X(4,5) = \frac{1}{\ell}(-6\xi+6\xi^{2})$

$X(2,2) = X(4,4) = (1-4\xi+3\xi^{2})$

$X(2,8) = X(4,10) = \frac{6}{\ell}(\xi-\xi^{2})$

$X(2,9) = X(4,11) = 3\xi^{2}-2\xi$

$X(5,5) = 1-10\xi^{3}+15\xi^{4}-6\xi^{5}$

$X(5,6) = \ell\xi(1-6\xi^{2}+8\xi^{3}-3\xi^{4})$

$X(3,7) = \ell^{2}\xi^{2}(1-3\xi+3\xi^{2}-\xi^{3})/2$

$X(3,12) = 10-15\xi+6\xi^{2}$

$X(5,13) = \ell\xi^{3}(-4+7\xi-3\xi^{2})$

$X(3,14) = \ell^{2}\xi^{3}(1-2\xi+\xi^{2})/2$

$X(6,3) = 30(-\xi^{2}+2\xi^{3}-\xi^{4})/\ell$

$X(6,6) = 1-18\xi^{2}+32\xi^{3}-15\xi^{4}$

$X(6,7) = \ell(2\xi-9\xi^{2}+12\xi^{3}-5\xi^{4})/2$

$X(6,12) = 30\xi^{2}(1-2\xi+\xi^{2})/\ell$

$X(6,13) = -12\xi^{2}+28\xi^{3}-15\xi^{4}$

$X(6,14) = \ell(3\xi^{2}-8\xi^{3}+5\xi^{4})/2$

$X(7,3) = 60\xi(-1+3\xi-2\xi^{2})/\ell^{2}$

$X(7,6) = (-36\xi+96\xi^{2}-60\xi^{3})/\ell$

$X(7,7) = 1-9\xi+18\xi^{2}-10\xi^{3}$

$X(7,12) = 60\xi(1-3\xi+2\xi^{2})/\ell^{2}$

$X(7,13) = (-24\xi+84\xi^{2}-60\xi^{3})/\ell$

$X(7,14) = (3\xi-12\xi^{2}+10\xi^{3})$

### 2.3 Strains

The linear strain displacement relations for a shell of revolution are expressed as [12].

$$
\begin{aligned}
\epsilon_s &= v_s + w\phi_s \\
\epsilon_\theta &= \frac{1}{r}(\dot{v} + v\sin\phi + w\cos\phi) \\
\epsilon_{s\theta} &= \frac{\dot{v}}{r} + v_s - \frac{v}{r}\sin\phi \\
K_s &= -w_{ss} - u\phi_{ss} - u_s\phi_s \\
K_\theta &= -\frac{\ddot{w}}{r^2} + \frac{\dot{v}}{r^2}\cos\phi - \frac{\sin\phi}{r}(w_s+u\phi_s) \\
K_{s\theta} &= \frac{2}{r}\Big(-\dot{w}_s - \dot{u}\phi_s + \frac{\dot{w}}{r}\sin\phi + v_s\cos\phi - \frac{v}{r}\sin\phi\cos\phi\Big)
\end{aligned}
\tag{9}
$$

where superscripts . and .. denote first and second derivatives respectively with respect to $\theta$ and subscripts s and ss for u, v, w and $\phi$ denote first and second derivatives with respect to s.

Using equations (4) and (9) the reference surface strains and curvatures can also be expressed as a Fourier series in $\theta$ as follows.

$$
\begin{Bmatrix} \epsilon_s \\ \epsilon_\theta \\ \epsilon_{s\theta} \\ K_s \\ K_\theta \\ K_{s\theta} \end{Bmatrix}
=
\begin{Bmatrix} \epsilon_s^o \\ \epsilon_\theta^o \\ \epsilon_{s\theta}^o \\ K_s^o \\ K_\theta^o \\ K_{s\theta}^o \end{Bmatrix}
+ \sum_{J=1}^{N}
\left[
\begin{Bmatrix} \epsilon_s^J \cos J\theta \\ \epsilon_\theta^J \cos J\theta \\ \epsilon_{s\theta}^J \sin J\theta \\ K_s^J \cos J\theta \\ K_\theta^J \cos J\theta \\ K_{s\theta}^J \sin J\theta \end{Bmatrix}
+
\begin{Bmatrix} \bar{\epsilon}_s^J \sin J\theta \\ \bar{\epsilon}_\theta^J \sin J\theta \\ \bar{\epsilon}_{s\theta}^J \cos J\theta \\ \bar{K}_s^J \sin J\theta \\ \bar{K}_\theta^J \sin J\theta \\ \bar{K}_{s\theta}^J \cos J\theta \end{Bmatrix}
\right]
\tag{10}
$$

The coefficients in the above series are given by the following matrix equations.

$$
\begin{Bmatrix} \epsilon^J \\ K^J \end{Bmatrix} = [Y^J]\{\Delta^J\} \quad J = 0,1,2,3\ldots N_c \tag{11}
$$

$$
\begin{Bmatrix} \bar{\epsilon}^J \\ \bar{K}^J \end{Bmatrix} = [\bar{Y}^J]\{\bar{\Delta}^J\} \quad J = 1,2,3,\ldots N_b \tag{12}
$$

where $\begin{Bmatrix} \epsilon^J \\ K^J \end{Bmatrix}^T = \{\epsilon_s^J\ \epsilon_\theta^J\ \epsilon_{s\theta}^J\ K_s^J\ K_\theta^J\ K_{s\theta}^J\}$

and similar expression for $\begin{Bmatrix} \bar{\epsilon}^J \\ \bar{K}^J \end{Bmatrix}^T$ . Matrices $[Y^J]$ and $[\bar{Y}^J]$ are given in Appendix II.

Substituting expressions (5) and (6) in equations (11) and (12) respectively, the strain components can be directly expressed in terms of nodal variables $\{q^J\}$ and $\{\bar{q}^J\}$ .

### 2.4 Strain Energy and Stiffness Matrices

The elastic strain energy U stored in an element of a laminated composite shell during deformation is given by

$$
U = \frac{1}{2}\int_{\xi=0}^{1}\int_{\theta=0}^{2\pi} L\,[\{\epsilon\}^T[A]\{\epsilon\} + \{\epsilon\}^T[B]\{k\} + \{k\}^T[B]\{\epsilon\} + \{k\}^T[D]\{k\}]\, r(\xi)\, d\xi d\theta \tag{13}
$$

where [A], [B] and [D] are membrane, bending-stretching coupling and bending stiffness matrices of the composite laminate. The elements [A], [B], and [D] matrices can easily be calculated provided the unidirectional lamina elastic constants and appropriate lamination parameters are known [13].

On substituting for $\{\epsilon\}$ and $\{K\}$ in terms of $\{q^J\}$ and $\{\bar{q}^J\}$ from equations (5), (6), (11), and integrating with respect to $\theta$ from 0 to $2\pi$ the expression for U can be written in terms of the nodal degrees of freedom $\{q^o\}$ , $\{q^J\}$ and $\{\bar{q}^J\}$ of the element as follows.

$$U = \frac{1}{2}\{q^0\}^T[K^0]\{q^0\} + \frac{1}{2}\Sigma\{q^J\}^T[K^J]\{q^J\} + \frac{1}{2}\Sigma\{\bar{q}^J\}^T[\bar{K}^J]\{\bar{q}^J\} + \frac{1}{2}\Sigma\{q^J\}^T[CK^J]\{\bar{q}^J\} \qquad (14)$$

## Appendix - II

Matrix $[Y^J]$ and $[\bar{Y}^J]$ in the relations

$$\begin{Bmatrix} \epsilon^J \\ K^J \end{Bmatrix} = [Y^J]\{\Delta^J\}, \quad J = 0,1,2 \ldots N_{CT} \qquad \text{(Eqn. 11)}$$

$$\begin{Bmatrix} \bar{\epsilon}^J \\ \bar{K}^J \end{Bmatrix} = [\bar{Y}^J]\{\bar{\Delta}^J\}, \quad J = 1,2 \ldots N_{sf} \qquad \text{(Eqn. 12)}$$

$[Y^J]$ is as follows:

$$\begin{bmatrix} 0 & 1 & 0 & 0 & \phi_s & 0 & 0 \\ \frac{\mathrm{Sin}\phi}{r} & 0 & \frac{J}{r} & 0 & \mathrm{Cos}\phi & 0 & 0 \\ \frac{-J}{r} & 0 & \frac{-\mathrm{Sin}\phi}{r} & 1 & 0 & 0 & 0 \\ -\phi_{ss} & -\phi_s & 0 & 0 & 0 & 0 & -1 \\ \frac{-\mathrm{Sin}\phi}{r}\phi s & 0 & \frac{J}{r^2}\mathrm{Cos}\phi & 0 & \frac{J^2}{r^2} & \frac{\mathrm{Sin}\phi}{r} & 0 \\ \frac{2J}{r}\phi s & 0 & \frac{-2\mathrm{Sin}\phi\,\mathrm{Cos}\phi}{r} & \frac{2\mathrm{Cos}\phi}{r} & \frac{2J\,\mathrm{Sin}\phi}{r^2} & \frac{2J}{r} & 0 \end{bmatrix}$$

where $[K^0]$, $[K^J]$ and $[\bar{K}^J]$ are the element elastic stiffness matrices corresponding to the constant part, symmetric part of the Jth harmonic and anti-symmetric part of the Jth harmonic respectively in the Fourier series representation of the displacements, and $[CK^J]$ is a coupling stiffness matrix representing the coupling in the Jth harmonic between the two series in the displacement functions. Expressions for $[K^0]$, $[K^J]$, $[\bar{K}^J]$ and $[CK^J]$ are follows.

$$[K^0] = 2\pi\ell \int_{\xi=0}^{1} r(\xi)\, d\xi\, [X]^T [Y^0]^T \begin{bmatrix} A & B \\ B & D \end{bmatrix} [Y^0][X]$$

$$[K^J] = \pi\ell \int_{\xi=0}^{1} r(\xi)\, d\xi\, [X]^T [Y^J]^T \begin{bmatrix} A^* & B^* \\ B^* & D^* \end{bmatrix} [Y^J][X]$$

$$[\bar{K}^J] = \pi\ell \int_{\xi=0}^{1} r(\xi)\, d\xi\, [X]^T [\bar{Y}^J]^T \begin{bmatrix} A^* & B^* \\ B^* & D^* \end{bmatrix} [\bar{Y}^J][X]$$

$$[CK^J] = \pi\ell \int_{\xi=0}^{1} r(\xi)\, d\xi\, [X]^T [Y^J]^T \begin{bmatrix} A' & B' \\ B' & D' \end{bmatrix} [\bar{Y}^J][X] \qquad (15)$$

Matrices $[A^*]$, $[B^*]$ and $[D^*]$ are derived from matrices [A], [B] and [D] respectively by replacing elements $A_{16}$, $A_{26}$ in [A], $B_{16}$, $B_{26}$ in [B] $D_{16}$, $D_{26}$ in [D] b[illegible]ices $[A']$, $[B']$ and $[D']$ are derived from [A], [B] and [D] respectively by putting all elements other than $A_{16}$, $A_{26}$, $B_{16}$, $B_{26}$, $D_{16}$ and $D_{26}$ as zero.

It is clear from the last term of expression (14) for the elemental strain energy that for a general composite laminate the generalized nodal displacements $\{q^J\}$ and $\{\bar{q}^J\}$ corresponding to the symmetric and anti-symmetric components of displacement for a given harmonic number J are coupled through terms involving stiffness coefficients $A_{16}$, $A_{26}$ corresponding to inplane stretching shearing coupling, $D_{16}$, $D_{26}$ corresponding to bending twisting coupling and $B_{16}$, $B_{26}$ corresponding to stretching twisting (shearing bending) coupling. Fortunately, for a large class of practical composite laminates the coefficients $A_{16}$, $A_{26}$, $B_{16}$, $B_{26}$, $D_{16}$ and $D_{26}$ are either zero or small compared to the rest of the coefficients so that their influence is negligible. Under such circumstances the terms in the expression for U involving these parameters can be neglected, thus eliminating the coupling between $\{q^J\}$ and $\{\bar{q}^J\}$.

Minimization of the elemental strain energy (Eq.14) with respect to the nodal variables $\{q^0\}$, $\{q^J\}$ and $\{\bar{q}^J\}$ respectively yields the corresponding nodal force vectors $\{Q^0\}$, $\{Q^J\}$ and $\{\bar{Q}^J\}$ in the following form.

$$\{Q^0\} = [K^0]\{q^0\} \qquad (16)$$

$$\begin{Bmatrix} Q^J \\ \bar{Q}^J \end{Bmatrix} = \begin{bmatrix} K^J & CK^J \\ CK^{J\,T} & \bar{K}^J \end{bmatrix} \begin{Bmatrix} q^J \\ \bar{q}^J \end{Bmatrix} \qquad (17)$$

It is thus seen that for a general laminated element, for a given harmonic number J in the displacement functions, the corresponding generalized forces $\{Q^J\}$ and $\{Q^{-J}\}$ are functions of both $\{q^J\}$ and $\{q^{-J}\}$. However, when $A_{16}$, $A_{26}$, $B_{16}$, $B_{26}$ and $D_{16}$ and $D_{26}$ are either zero or small $[CK^J] = 0$ or its elements are small compared to those of [K] and [K`], and can be neglected.

For these cases $\{Q^J\}$ and $\{Q^{-J}\}$ are uncoupled and are given by

$$\{Q^J\} = [K^J]\{q^J\}$$

$$\{Q^{-J}\} = [K^{-J}]\{q^{-J}\} \qquad (18)$$

It is clear from eqns (17) and (18) that when the coupling effects are significant, the generalized coordinates $\{q^J\}$ and $\{q^{-J}\}$ corresponding to the cosine and sine series should be considered together. As a result, the number of degrees of freedom per element, the size of the stiffness matrix and consequently the number of final force displacement equations to be solved are twice those for the case when the coupling is zero or negligible (Eqn.16).

### 2.5 Stress Resultants

For arbitrarily laminated composite shells the membrane and bending stress resultants (Fig.2) are related to the reference surface strains and curvature changes by the following matrix equation (13).

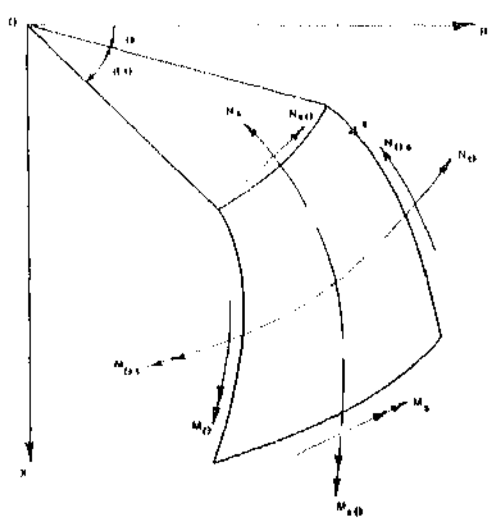

FIG 2. Membrane and Bending Stress Resultants

$$\begin{Bmatrix} N \\ M \end{Bmatrix} = \begin{bmatrix} A & B \\ B & D \end{bmatrix} \begin{Bmatrix} E \\ k \end{Bmatrix} \qquad (19)$$

Where $\begin{Bmatrix} N \\ M \end{Bmatrix}^T = \{N_s \; N_\theta \; N_{s\theta} \; M_s \; M_\theta \; M_{s\theta}\}$ (20)

combining eqns. (19) and (10), each of the stress and moment resultants can be expressed as follows.

$$N_s = N_s^o + \sum_{J=1}^{N_c} N_s^J \cos J\theta + \sum_{J=1}^{N_s} N_s^{-J} \sin J\theta + \sum_{J=1}^{N_c} N_s^{1J} \sin J\theta + \sum_{J=1}^{N_s} N_s^{-1J} \cos J\theta \qquad (21)$$

and similarly for $N_\theta$, $M_s$, and $M_\theta$.

$$N_{s\theta} = N_{s\theta}^o + \sum_{J=1}^{N_c} N_s^J \sin J\theta + \sum_{J=1}^{N_s} N_s^{-J} \cos J\theta + \sum_{J=1}^{N_c} N_s^{1J} \cos J\theta + \sum_{J=1}^{N_s} N_s^{-1J} \sin J\theta \qquad (22)$$

and similarly for $M_{s\theta}$.

Here,

$$\begin{Bmatrix} N^o \\ M^o \end{Bmatrix} = \begin{bmatrix} A & B \\ B & D \end{bmatrix} \begin{Bmatrix} E^o \\ k^o \end{Bmatrix}, \quad \begin{Bmatrix} N^J \\ M^J \end{Bmatrix} = \begin{bmatrix} A^* & B^* \\ B^* & D^* \end{bmatrix} \begin{Bmatrix} E^J \\ k^J \end{Bmatrix}, \quad \begin{Bmatrix} N^{-J} \\ M^{-J} \end{Bmatrix} = \begin{bmatrix} A^* & B^* \\ B^* & D^* \end{bmatrix} \begin{Bmatrix} E^{-J} \\ k^{-J} \end{Bmatrix}$$

$$\begin{Bmatrix} N^{1J} \\ M^{1J} \end{Bmatrix} = \begin{bmatrix} A^+ & B^+ \\ B^+ & D^+ \end{bmatrix} \begin{Bmatrix} E^J \\ k^J \end{Bmatrix} \; \& \; \begin{Bmatrix} N^{-1J} \\ M^{-1J} \end{Bmatrix} = \begin{bmatrix} A^+ & B^+ \\ B^+ & D^+ \end{bmatrix} \begin{Bmatrix} E^{-J} \\ k^{-J} \end{Bmatrix} \qquad (23)$$

combining eqns.(22), (23), (5), (6), (11) and (12) the stress resultants can be expressed in terms of the generalized nodal displacements of the element $\{q^J\}$ and $\{q^{-J}\}$.

### 2.6 Kinematically Consistent Loads

The externally applied loads on the element are first converted into a set of kinematically equivalent loads consistent with the element degrees of freedom using the principle of virtual work. The procedure for external normal pressure whose distribution may be asymmetric around the circumference is given here. The pressure $p_z$ is first decomposed into a series of harmonic functions around the circumference as follows.

$$p_z = p_z^o + \sum_{J=1}^{N_c} p_z^J \cos J\theta + \sum_{J=1}^{N_s} p_z^{-J} \sin J\theta \qquad (24)$$

The virtual work done by the pressure

$p_z$ acting over the entire element is obtained as

$$\text{virtual work} = \int_{\xi=0}^{1}\int_{\theta=0}^{2\pi} (f)_z \, \ell \, d\xi \, r \, d\theta \, . \, w \qquad (25)$$

On substituting for $p_z$ and $w$ from eqns. (24) and (4) respectively and integrating between the limits 0 to $2\pi$, the expression for the virtual work can be expressed as

$$\text{Virtual Work} = \{p^{o}\}^{T}\{q^{o}\} + \sum_{j=1}^{N_c}\{p^{j}\}^{T}\{q^{j}\} + \sum_{j=1}^{N_s}\{p^{-j}\}^{T}\{q^{-j}\} \qquad (26)$$

where $\{p^{o}\}^{T} = 2\pi\ell \int_{\xi=0}^{1} r(\xi)\, p_z^{o}(\xi) \{x_w\}^{T} d\xi$

$$\{p^{j}\}^{T} = \pi\ell \int_{\xi=0}^{1} r(\xi)\, p_z^{j}(\xi) \{x_w\}^{T} d\xi$$

$$\{p^{-j}\} = \pi\ell \int_{\xi=0}^{1} r(\xi)\, p_z^{-j}(\xi) \{x_w\}^{T} d\xi \qquad (27)$$

and $\{x_w\}$ is the coefficient matrix expressing contributions of the elemental degrees of freedom to the displacement $w^{*}$ and is given by

$$\{w^{j}\} = \{x_w\}^{T}\{q^{j}\} \quad j = 0,1,2 \ldots N_c$$

$$\{w^{-j}\} = \{x_w\}^{T}\{q^{-j}\} \quad j = 1,2,\ldots N_s \qquad (28)$$

From eqn.(26) it is clear that for a normal pressure distribution on the element, the kinematically consistent generalized load vectors corresponding to the elemental nodal variables $\{q^{o}\}$, $\{q^{j}\}$ and $\{q^{-j}\}$ are given by $\{P^{o}\}$, $\{P^{j}\}$ and $\{P^{-j}\}$ respectively. Similar expressions can also be derived for generalized load vectors corresponding to externally applied inplane loads.

## 2.7 Assembly and Solution

In the small displacement analysis each harmonic component of the applied load is related only to the nodal displacements of the same harmonic through a corresponding stiffness matrix. Thus there is no coupling between different harmonics (that is, between $i^{th}$ and $j^{th}$ harmonics). In practice therefore, there are only as many harmonic terms in the displacement series as it is necessary for an accurate description of the applied load. Hence it is possible to assemble the stiffness matrix of the complete structure for each harmonic J and find the solution separately. When all the element matrices are assembled and boundary conditions incorporated the resulting discrete system field equations can be represented in the following form.

$$[K^{J}]\{\rho^{J}\} = \{F^{J}\} \qquad (29)$$

where $\{\rho^{J}\}$ is the vector of unknown generalized nodal displacements composed of sub-vectors $\{q^{J}\}$ at the various nodal circles taking into account the boundary conditions, $[K^{J}]$ is the structural stiffness matrix which is symmetric, positive definite and strongly banded and $\{F^{J}\}$ is the vector of generalized kinematically consistent loads.

Once the global nodal displacements $\{\rho^{J}\}$ corresponding to the $J^{th}$ harmonic are determined from the solution of equation (29) it is possible to go back to the elemental level by evaluating the sub-vectors $\{q^{J}\}$ giving the elemental nodal variables for each element. Eqns. (11) and (12) then give the reference surface strains and curvature changes and the stress resultants are obtained using eqns (21) to (23). Knowing the results for each harmonic, the circumferential variation of any parameter may be obtained from the harmonic function representation.

The formulation described above was programmed on IBM 370 computer using FORTRAN IV language. The integrals involved in the stiffness matrix terms Eqn. (19) and the generalised load vectors Eqn. (27) are evaluated using numerical quadrature integration. The force displacement Eqn. (29) for each harmonic are solved using Choleski square root decomposition algorithm for fixed bandwidth problems.

## 5 Applications to Practical Problems

The method presented is first verified by applying it to a cooling tower (Fig. 3) presented in ref.[8] and comparing the results. Fig 4a and b shows a typical comparison, where the agreement is found to be very good.

FIG 3(a). Hyperbolic Cooling Tower

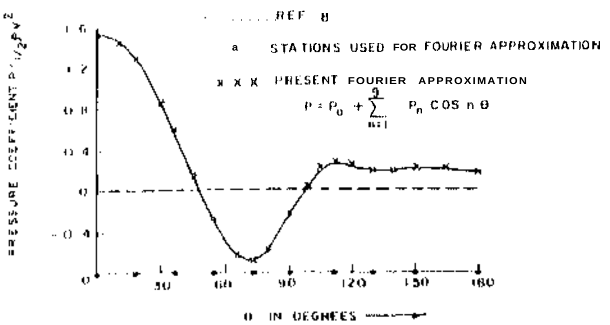


FIG 3(b). Circumferential Distribution of Wind Pressure

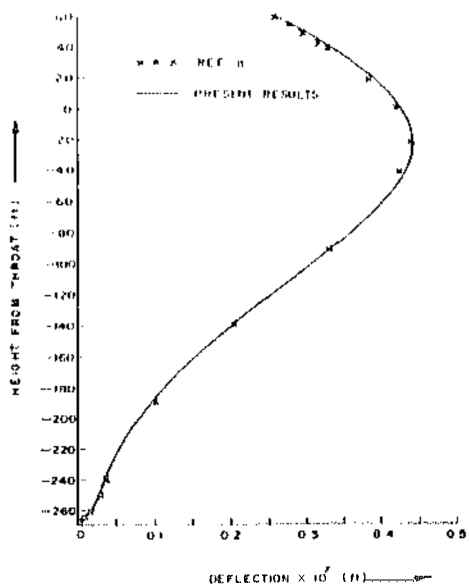


FIG 4(a). Radial Deflection At θ = 0°

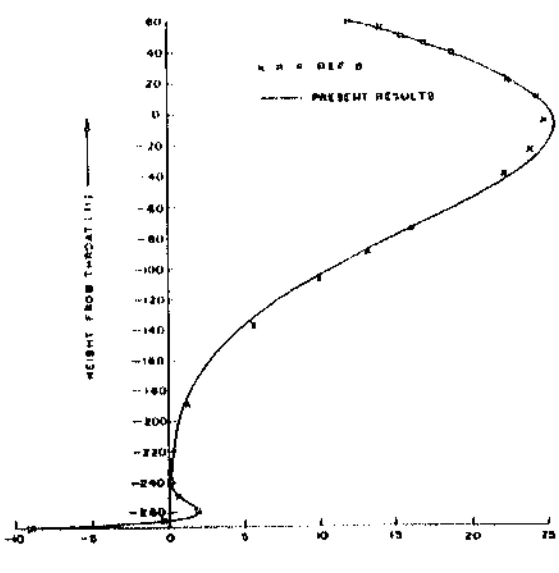


FIG 4(b). Variation of $M_\theta$ at $\theta = 0^\circ$

Solutions are obtained for a fibre reinforced composite cone and a tangent ogive shell, subjected to asymmetric wind loads. These are described below.

### 3.1 Cone

Fig 5a shows geometry of the cone. It is assumed to be fabricated using layers of resin impregnated woven glass cloth. Typical properties of *a* woven glass laminate used in the analysis are given in Table 1 [14]. The circumferential wind pressure distribution, assumed to be the same at all stations along the length, is shown in fig 6a and its Fourier series representation is also indicated. For analytical purposes the L and T directions of the fibre lay-ups are assumed to be coincident with the meridional and circumferential directions.

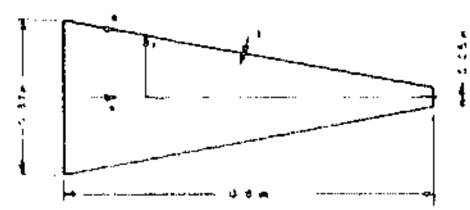

FIG 5(a). Geometry of Cone

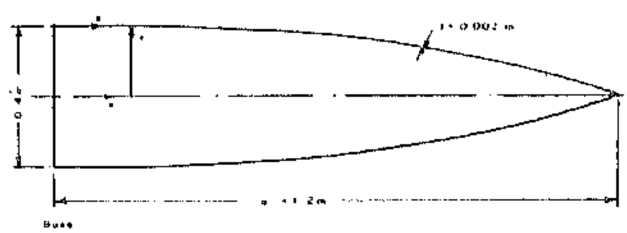


FIG 5(b). Geometry of Tangent Ogive

The cone is assumed to be rigidly supported at the base and free at the tip. A total of 30 elements are used in the finite element idealization, the nodes being closer near the base to take care of sharp variations due to bending effects. Typical results for displacement and stress resultant variations for cones with wall thickness varying from 1.0 to 3.0 mm are given in Fig 8 to 11. The parameters presented in all the figures correspond to a unit value of wind dynamic pressure q.

Fig 8a shows the variation of radial deflection along the windward generator (i.e. θ = 0° ), and Fig 8b shows its circumferential variation at the free end. The deflection is inwards (negative) at the windward side, its maximum value occuring at the free end, but becomes outwards (positive) at the leeward side (i.e. for θ greater than about 70° ).

**Table 1**

**Mechanical Properties of Woven glass Laminate (Ref.14)**

| | | |
|---|---|---|
| Resin content | = | 31% |
| $E_L$ | = | $25.993 \times 10^6 KN/m^2$ |
| $E_T$ | = | $19.995 \times 10^6 KN/m^2$ |
| $G_{LT}$ | = | $4.895 \times 10^6 KN/m^2$ |
| $\mu_{LT}$ | = | 0.1644 |
| $\sigma^L{}_u$ | = | $309.24\ MN/m^2$ |
| $\sigma^T{}_u$ | = | $216.36\ MN/m^2$ |
| $\tau_{LT}$ | = | $21.72\ MN/m^2$ |

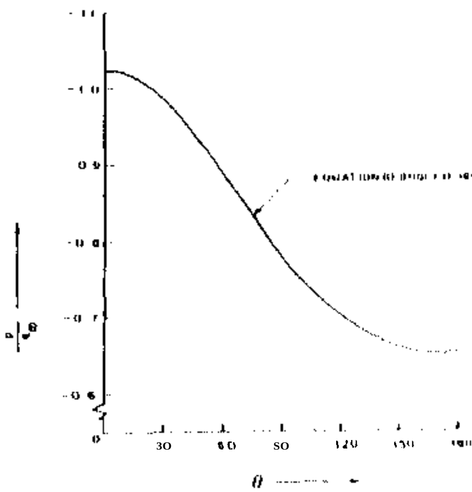

FIG 6(a). Circumferential Pressure Distribution of Cone

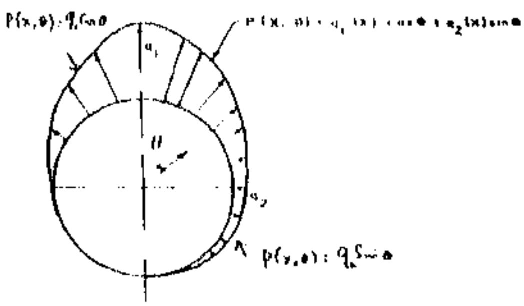

FIG 6(b). Circumferential Pressure Distribution of the Ogive

The variations of stress and moment resultants $N_s$, $M_s$, $N_\theta$ and $M_\theta$ along the windward generator are shown in figures 9a, b and 10a, b respectively. $N_s$, $M_s$ and $N_\theta$ assume their largest magnitude near the base whereas the maximum value of $M_\theta$ occurs near the free end and the location of this maximum shifts away from the free end as the wall thickness increases.

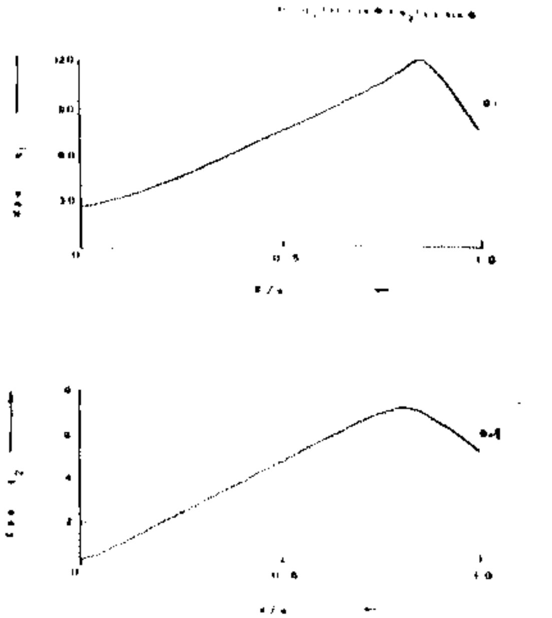

FIG 7. Variation of Pressure Along the Length of the Ogive

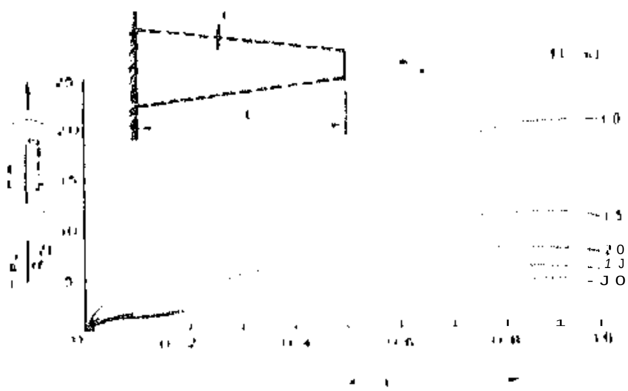

FIG 8(a). Radial Deflection Along Windward Generator

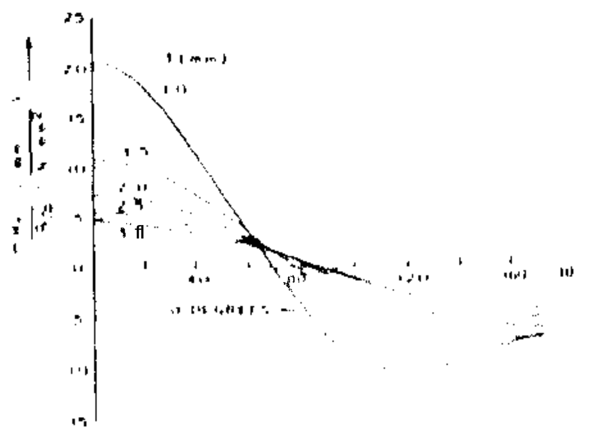

FIG 8(b). Radial Deflection at the Free End

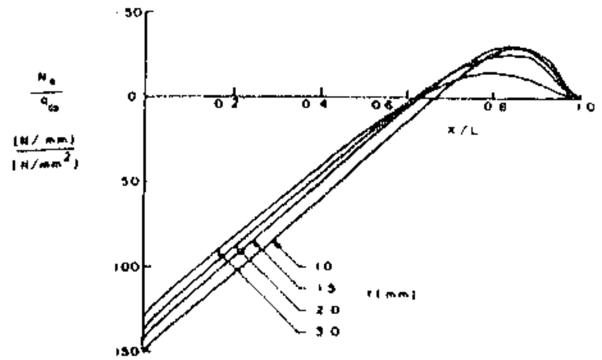


FIG 9(a). $N_s$ Variation Along Windward Generator (9=0°)

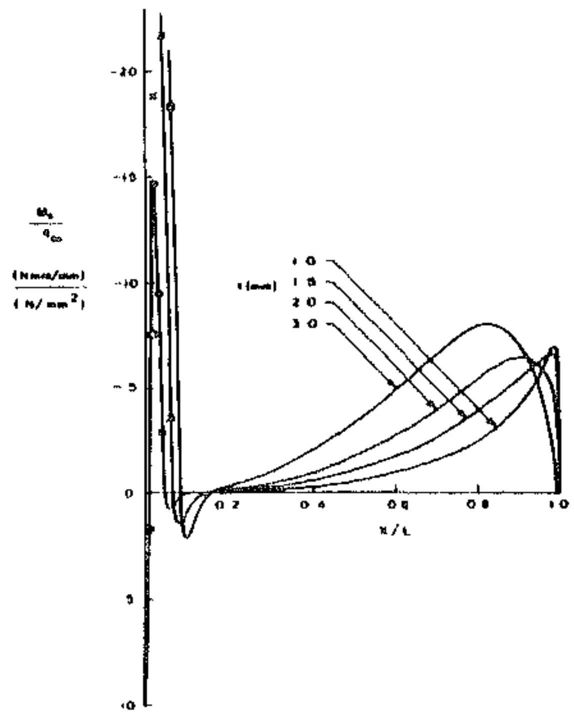


FIG 9(b). $M_s$ Variation Along Windward Generator (Θ=0°)

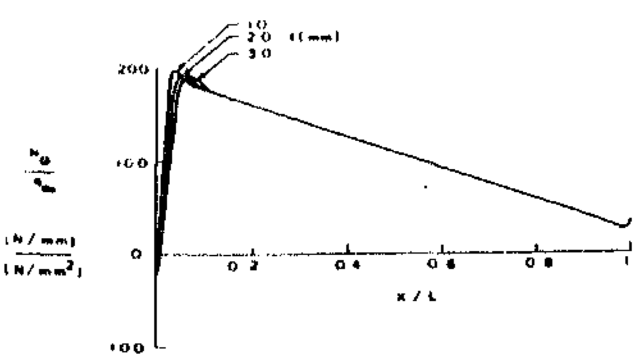


FIG 10(a). $N_\Theta$ Variation Along Windward Generator (Θ=0°)

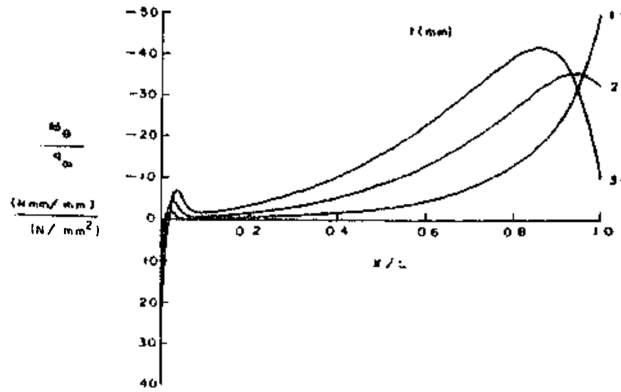


FIG 10(b). $M_\Theta$ Variation Along Windward Generator (Θ=0°)

Fig 11a and b depict the circumferential variation of $M_s$ and $N_s$ respectively at the fixed end. $N_s$ is tensile near the region Θ = 0°, but becomes compressive for Θ, greater than about 55°, whereas the bending stress resultant $M_s$ remains positive all round the circumference causing tensile bending stresses in the outer fibres and compressive stresses in the inner fibres.

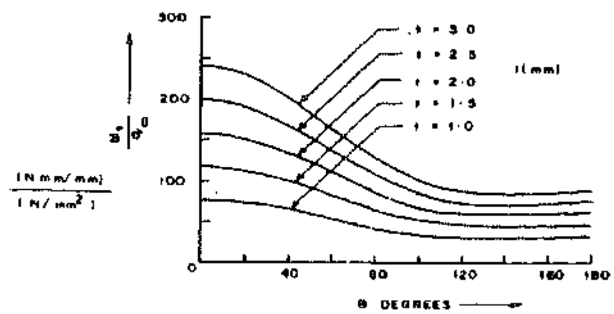


FIG 11(a). Variation of $M_s$ at Root End

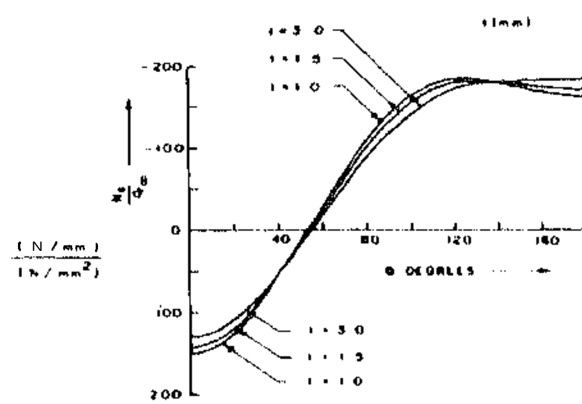


FIG 1Kb). Variation of $N_s$ at Root End

### 3.2 Tangent Ogive Shall

Fig 5a shows the geometry of the tangent ogive. As in the case of the cone example, the shell is assumed to be fabricated using layers of resin impregnated woven glass cloth, the typical properties of which are given in Table I. Once again the L and T directions of the fibre layup are assumed to coincide with meridional and circumferential directions.

The external pressure acting on the shell is assumed to be of the form $q_1(X)\cos\theta + q_2(X)\sin\theta$. pressure distribution along the circumference as represented by a combination of sine and cosine distributions is depicted in Fig 6b. Variation of the multipliers $q_1(x)$ and $q_2(x)$ along the length of the generator is shown in Fig 7. The Fourier expansion of the pressure distribution can readily be written as

$$p(X,\theta) = \frac{1}{2}p_0(x) + \sum_{J=1}^{\infty} p_J(x)\cos J\theta + \sum p_J^-(x)\sin J\theta$$

$$\text{where}\quad p_0 = \frac{2}{\pi}(q_1+q_2),\; p_1 = \frac{q_1}{2},\; p_1^- = \frac{q_2}{2} \qquad (30)$$

$$p_J = \frac{-2q_1(-1)^{J/2}}{\pi(J^2-1)} - \frac{2q_2}{\pi(J^2-1)} \quad \text{for } J = 2, 4, 6, 8, \ldots$$

$$p_J^- = 0 \text{ for } J \geq 2, \quad p_J = 0 \quad J = 3, 5, 7, \ldots$$

The shell is assumed to be rigidly fixed at the base and free at the tip. 50 elements are used to idealize the shell,

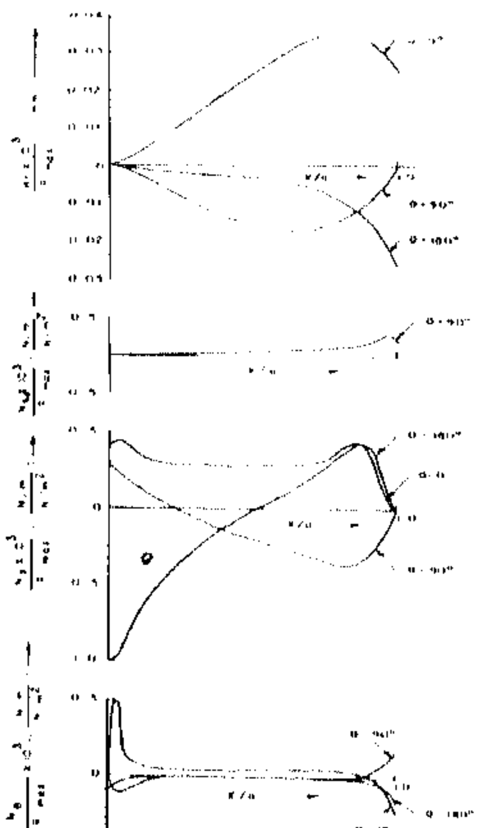

FIG 12. Radial Displacement and Membrane Strain Resultants $N_s$, $N_\theta$ and $N_{s\theta}$ in Ogive

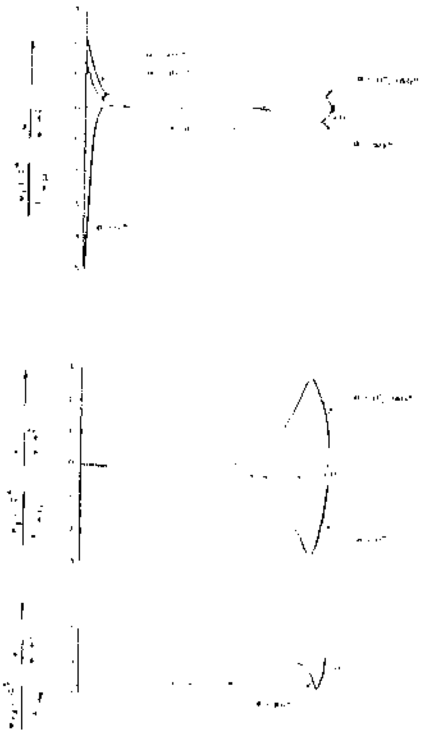

FIG 13. Bending Moment Resultants in the Ogive

Typical results of the analysis are presented in Figs 12 and 13 along the generators at 0, 90° and 180°.

Fig 12 gives the radial displacement w along the generators. It is outward at θ = 0, reaching a maximum value at about 0.24 m from the tip. Radial deflection at θ = 180° is inward with its maximum at the tip. At θ = 90°, it is inward and reaches its maximum at about 0.38 m from the tip.

Fig 12 also gives the distributions of membrane stress resultants $N_s$, $N_\theta$ and $N_{s\theta}$ along the generators. $N_\theta$ at θ = 0 will be tensile near the tip and becomes compressive at the fixed end. $N_\theta$ at θ = 90° shows a reverse effect. $N_\theta$ at 180° remains tensile throughout the generator. $N_s$ in the fixed end is compressive, becomes tensile at θ = 90° and again compressive at θ = 180°. However, the magnitude of $N$ at the root is quite small. Fig 13 shows the distribution of bending moment resultants $M_s$, $M_\theta$ and $M_{s\theta}$ along the generators. $M_s$ reaches its maximum value at the fixed end, while for $M_\theta$ maximum occurs approximately at 0.08m from the other end. At the fixed end $M_s$ causes compressive bending stress at θ = 0 and tensile bending stresses at θ = 90° and 180° in the outer fibres. Near the free end $M_s$ and $M_\theta$ cause tensile bending stresses for θ = 0 and 180° and compressive bending stresses for θ = 90° in the outer fibres. As can be seen from Fig 7 magnitude of $q_2$ is comparatively less than that of $q_1$ and the influence of the term $q_1\cos\theta$ in the expression for pressure is seen to be predominant in all the distributions.

## 4 Conclusions

An axisymmetric laminated shell finite element: is used for the static analysis of laminated composite shells of revolution subjected to asymmetric loading. A Fourier edxpansion is used to represent the circumferential variation of the loading and the resultant displacements. The examples considered are a cone and a tangent ogive shell made of glass reinforced composite and subjected to wind pressure loading. The analysis can also be used for the case of inertial and thermal loading.

## 5 Acknowledgements

The authors wish to thank Dr. V. Lakshminarayana, Scientist, Structures Division for many valuable suggestions and discussions, and Dr. B.R. Somashekar, Head, Structures Division for his keen interest and encouragement.

## References

1 Pandovan, J, and Lestingi, J.F., "Mechanical Behaviour of Fibre Reinforced Cylindrical Shells", AIAA Journal, Vol. 10, No.9, Sept: 1972, p 1239-1241.

2 Pandovan, J, and Lestingi, J.F., "Complex Numerical Integration Procedure for Static Loading of Anisotropic Shells of Revolution", Computers and Structures, Vol. 4, No.6, 1974, p 1159-1172.

3 Viswanath, S., and Lakshminarayana, H.V., "Application of the finite element method to the analysis of laminated composite shell structures", Proc. of Symp. on application of computer methods in Engineering, Vol. 11, Univ. of South California, USA, Aug 1977.

4 Witmer, F.A., and Kotanchik, J.J., "Progress Report on Discrete Element Elastic-Plastic Analysis of Shells of Revolution Subjected to Axisymmetric and Asymmetric Loading", Proc. Second Conf. on Motrix Method in Structural Mechanics, AFFDL-TR-68-150-1341-1453, 1969.

5 Brombolich, L.J., and Gould, P.L., "Finite Element Analysis of Shells, of Revolution by Minimization of the Potential Energy Function", Proc. of the Symp. on Application of Finite Element Methods in Civil Engg., Vanderbilt Univ., Nov 1969.

6 Dawe D.J., "Curved Finite Elements in the Analysis of Shell Structures". Proc. First Intl.. Conf. SMIRT, Berlin, Vol. 7 1971.

7 Gallagher, R.H., "Applications of Finite Element Analysis" Recent Advances in Computational Methods in Structural Mechanics and Design, U.A.H. Press, 1972.

8 Chan, A.S.L., and Firmin, A., "The Analysis of Cooling Towers by the Matrix Finite Element Method, Part II, Small Displacements". The Aeronautical Journal, Vol. 74, No. 718, October 1970.

9 Grafton, P.E., and Strome, D.R., "Analysis of Axisymmetrical Shells by the Direct Stiffness Method", AIAA Journal, Vol. 1, No. 10, October 1963, p 2342-2347.

10 Pandovan, J., "Quasi-Analytical Finite Element Procedures for Axisymmetric Anisotropic Shells and Solids". Computers and Structures, Vol. 4, 1974, p 467-483.

11 Lakshminarayana, H.V., "Finite Element Analysis of Laminated Composite Shell Structures, Part I: Static Analysis". NAL-TM-ST-403/170-77, Sept 1977.

12 Novozhilov, V.V., "The Theory of Thin Shells", II Edition, Noordhoff 1964.

13 Calcote, L.R., "The Analysis of Laminated Composite Structures", Van Nostrand, New York, 1967.

14 Ramesh Chandra, Kumar, M., Viswanathan K.S., "Experimental Characterisation of E glass - epoxy and E-glass phenolic Composites", NAL-TM-ST-404-200-78.